Selective laser melting of Al6061 alloy: Processing, microstructure, and mechanical properties

Jinliang Zhang, Bo Song ∗, Lei Zhang, Jie Liu, Yusheng Shi

State Key Laboratory of Materials Processing and Die & Mould Technology, Huazhong University of Science and Technology, Wuhan 430074, China

*Corresponding author: bosong@hust.edu.cn

Abstract

Selective laser melting (SLM) is considered as one of the most promising additive manufacturing (AM) technologies. Aluminum alloy is of wide application potentiality due to their high specific strength and heat resistance. In this study, Al6061 alloy was prepared via selective laser melting (SLM) and densification, microstructure and properties were investigated systematically. It was found that process parameters including laser power and scanning rate have a great effect on the forming quality and the porosity of the samples. The α-Al phase is observed in XRD results and (200) is the preferable orientations of α-Al crystal in the SLM process. The microstructure can be divided into three areas: fine grained area, coarse grained area and heat affected area. As for the nanohardness, with the increase of laser power, the elastic modulus and hardness of SLM aluminum alloy show the trend of increasing first and then decreasing, and with the increase of scanning speed, the hardness of SLMed aluminum alloy is gradually reduced. With the increasing laser power and decreasing scanning rate, the elastic modulus and hardness of the samples increased first and then decreased.

Keywords: Selective laser melting, Aluminum alloys, Microstructure, Densification, Mechanical property.

Introduction

Aluminum alloy has a large number of applications in the aviation, aerospace, automobile, naval and other industries due to low density, high strength-to-weight ratio, good corrosion resistance and good electrical and thermal conductivity [1-3]. At present, aluminum alloys are mainly fabricated using traditional methods such as casting, forging and extrusion [4]. Although the traditional cast aluminum alloy has been widely used, there are still many problems in the process of production and use. The coarse microstructure due to the low cooling rate and metallurgy defects lower the mechanical properties of the parts. In addition, the traditional process, from the casting ingot to the machine forming, to the final parts, requires a lot of process to complete with a low utilization of raw materials. Selective laser melting (SLM), as a as one of the most promising additive manufacturing (AM) technologies, has a unique advantage in forming parts with complex structures. The high cooling rate inhibites the grain growth and segregation of alloying elements which helps improve the mechanical properties [5].

Corresponding authors. Tel.: +86 15927261681.
E-mail addresses: bosong@hust.edu.cn (B. Song)

Recently, many studies have been carried out on the selective laser melting of AlSi10Mg and AlSi12 alloys for their near-eutectic composition and good casting properties. Noriko et al. [6] studied the effect of SLM process parameters on porosity in AlSi10Mg alloy components. It was found that the interaction among the laser power, scanning rate, and the scanning interval have a major influence on the the porosity of the samples. KG Prashanth et al. [7] investigated the influence of annealing process on the microstructure and tensile properties of Al-12Si. The results show that the mechanical properties of the samples can be adjusted by proper annealing treatment to achieve a combination of high strength and ductility. Wei Li et al. [8] systematically studied the effect of solution treatment and artificial aging heat treatment on the microstructure and mechanical properties of AlSi10Mg alloy parts produced by SLM. Studies have shown that the microstructure and mechanical properties of SLM-processed AlSi10Mg alloys can be tailored by proper solution treatment and artificial aging heat treatment. Shafaqat et al. [9] studied the cyclic fatigue and fatigue crack propagation behavior of Al-Si12 alloys, and effect of the substrate heating on the fatigue and crack growth behavior is investigated. In addition to the Al-Si series alloys, other aluminum alloys have been studied at in recent years. A.B. Spierings [10] studied the microstructure characteristics of Sc and Zr modified Al-Mg alloys and it was found that Al-Mg-Sc-Zr alloy shows excellent mechanical performance. Zhang Hu et al. [11] found that a dense Al-Cu-Mg alloy sample (99.8%) could be obtained using the laser energy density threshold value of 340 J / mm3. The ultimate tensile strength and yield strength are 402 MPa and 276 MPa, respectively. The research on SLM-fabricated aluminum alloys has shown that this technology has a good application prospect in material forming and processing. We can produce more complex and superior aluminum alloy parts than the traditional casting process by setting appropriate process parameters. However, SLM-fabricated aluminum alloy has many technical difficulties compared with other alloys, especially the high porosity and cracking level.

In this study, 6061 aluminum alloy, which is well known for its good corrosion resistance and toughness and medium strength, was used for SLM. First, the processing parameters were optimized in order to obtain high quality printed samples by SLM. Afterward, the microstructure, phase constituents and properties of SLM samples were studied.

Experimental Procedure

The Al6061 powder used in the SLM experiment was prepared under Ar atmosphere by gas atomization. The powder composition is shown in Table 1. Fig. 1(a) and (b) show the sphere morphology and particle size distribution of Al6061 powder particles, respectively. The distribution accord with Gaussian distribution with an average particle size of 34.8 μm. Before SLM process, the powder was dried in a vacuum oven at a temperature of 80 °C for 6 h.

Table 1. Chemical composition of 6061 alloy (wt %)

Mg	Si	Cu	Cr	Fe	Zn	Mn	Ti	Al
1.01	0.72	0.29	0.24	0.16	0.02	0.08	<0.01	Bal.
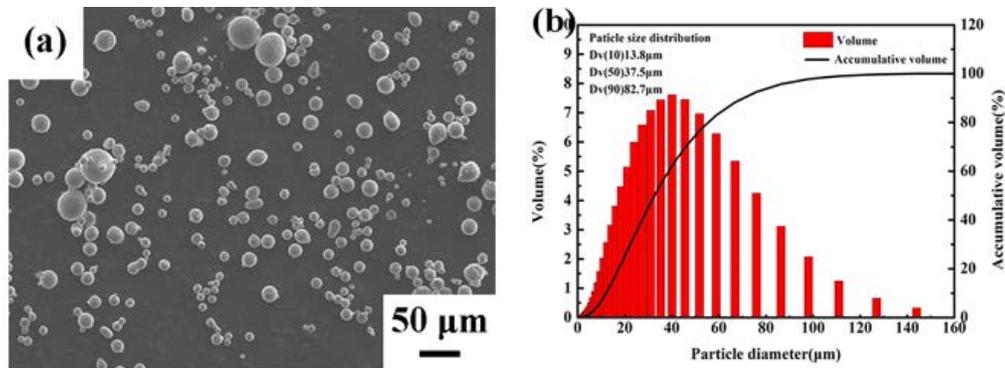
Fig. 1. (a) Morphology and (b) particle size distribution of Al6061 powder particles

All parts were made on the self-developed HRPM-II type SLM machine. This SLM installation is equipped with an Yb: YAG fibre laser, which can reach a maximum power of 400 W in continuous mode. The intensity distribution can be assumed to be Gaussian. Based on a series of preliminary experiments, the SLM parameters were fixed as follows: laser power of 240-360 W with an interval of 40 W, scanning speed of 450-900 mm/s with an interval of 150 mm/s, layer thickness of 0.05 mm, hatch spacing of 0.17 mm. The diagram of scanning strategy is shown in Fig. 2(a). The scanning direction is rotated by 90° after each layer. Bulk specimens with dimensions of 10 mm × 10 mm × 10 mm were produced, as shown in Fig. 2(b).
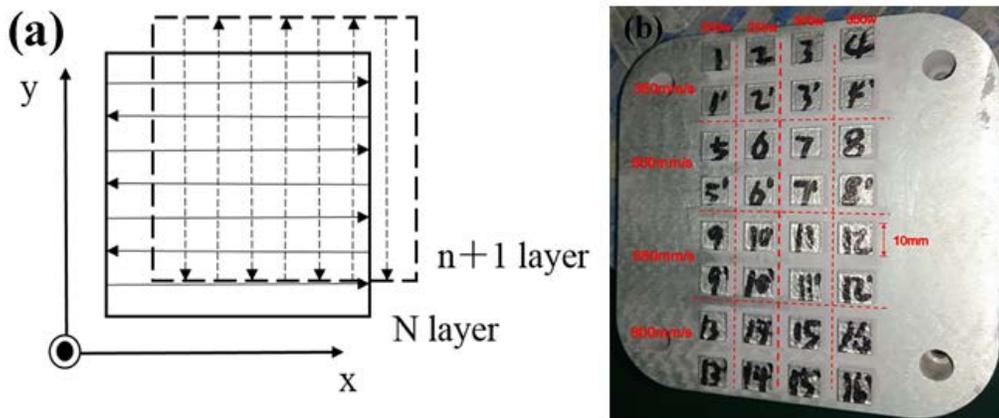
Fig. 2. (a) The diagram of scanning strategy; (b) SLM-processed specimens

A laser diffraction particle size analyzer (Mastersizer 3000, Worcestershire, United Kingdom) was applied to investigate the particle size distribution of Al6061 powders. The as-polished samples were etched in Keller reagent (2.5mL HNO_3, 1.5mL HCL, 1mL HF and 95 mL H_2O) for 15-20 s prior to microstructural characterization using a field emission scanning electron microscope (SEM, Quanta650 FEG, USA) fitted with an energy dispersive spectroscopy detector (EDX). The phases of the bulk specimens were identified through X-ray diffraction (XRD-7000) analyses, which were performed with a Cu K_α radiation source at 40 kV and 30 mA; the continuous scan mode was used and the scan rate was 5°/min.

The porosity calculated by 10 pictures of specimen morphology were used to express the density of specimens. Nanoindentation tests on the polished sections of SLM parts were performed using a TI750 nanoindentation tester (Hysitron, America) at room temperature. A loading–

unloading test mode was used and a test force 6000 µN, a loading speed 1.200 mN/s and a hold time 2 s were chosen.

Results and Discussion

Densification

The porosity of the samples were calculated using the Image J software. Fig. 3 shows the optical microscope picture of polished surfaces of the samples.
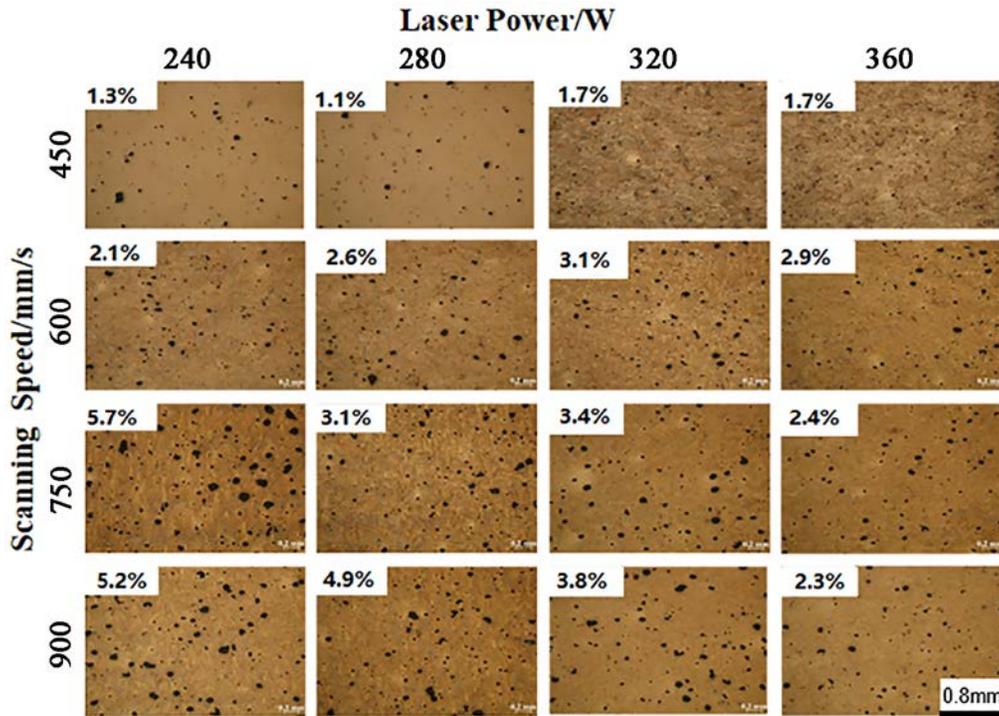
Fig. 3. Optical microscope picture of polished surfaces of the samples

The input laser energy per unit volume in the SLM forming process can be represented by the line laser energy density ψ (J/mm), as Equation 1:

$$\psi = P/(v*h*d) \tag{1}$$

Where P is the laser power (W), v is the scanning rate (mm/s), h is the hatch spacing and d is the layer thickness. It was determined that the density of the SLM machined parts is roughly an exponential function of the laser energy density incident on the powder bed. Specific formulas such as formulas [12, 13]:

$$\rho = C_1 - C_{2*}e^{-K\psi} \tag{2}$$

Where C_1 and C_2 and K (densification coefficient) are constants that related to specific materials. According to the empirical formula above, the fitting curve of the relationship between the line laser energy density and relative density is shown in Fig. 4. It can be seen that within the range of selected processing parameters, the density of the sample increases with the increase of the line

laser energy density, and the porosity is 2% until the line laser energy density is 85 J/mm. When the line laser energy density is high enough, the powder particles can fully melt and produce sufficient liquid metal to fill pores. Besides, the high temperature of the molten pool can reduce the melt viscosity and surface tension, improve the wettability of the melt with the solidified layer thus forming a good metallurgical bond and lowering the porosity.

$$D=0.984-0.037\exp(-0.064E+2.117)$$
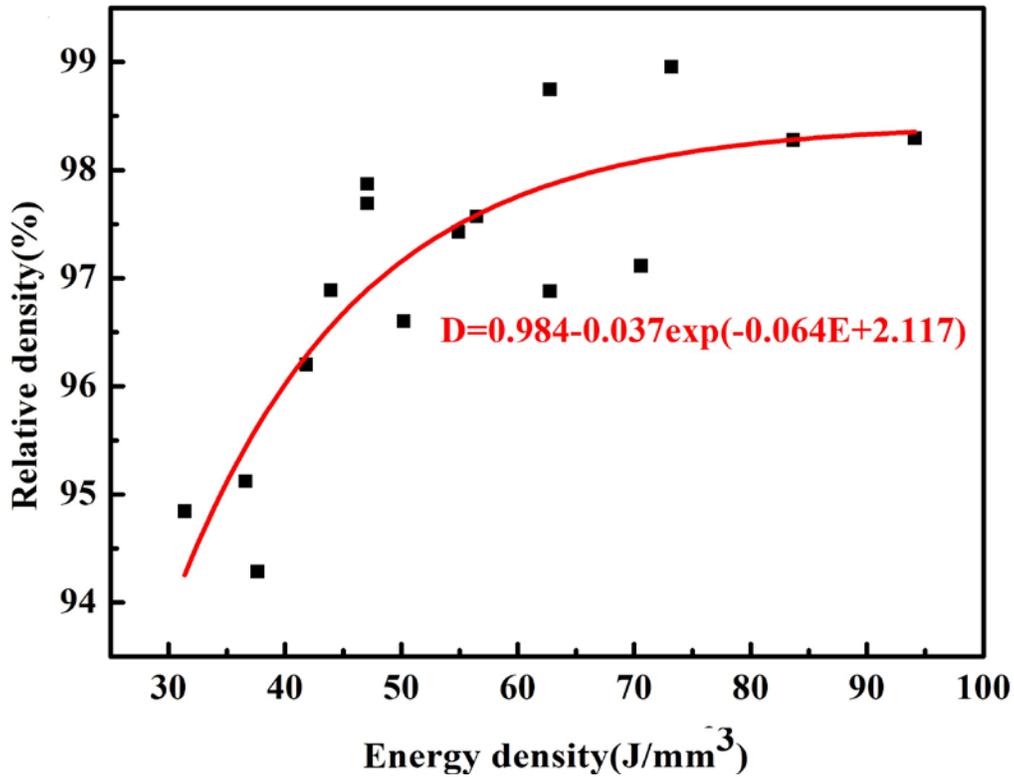
Fig. 4. Fitting curve of the relationship between the line laser energy density and relative density

Phase identification and microstructure analysis

Fig. 5 shows α-Al is the only phase in the raw powder and SLM-processed samples. No other phase such as Si or Mg_2Si was detected. This indicates that the α-Al phase in the original powder was retained during the SLM process. It can be speculated that rapid heating and rapid cooling in the SLM process increase the solid solubility limit of Si and Mg in the alloy and suppress the precipitation of the second phase. The relative intensity of the Al (200) Braggs peak is much stronger than that of original powder, indicating the much stronger (200) texture. The (200) texture is due to the preferential solidification in the 〈100〉 direction of fcc structure.
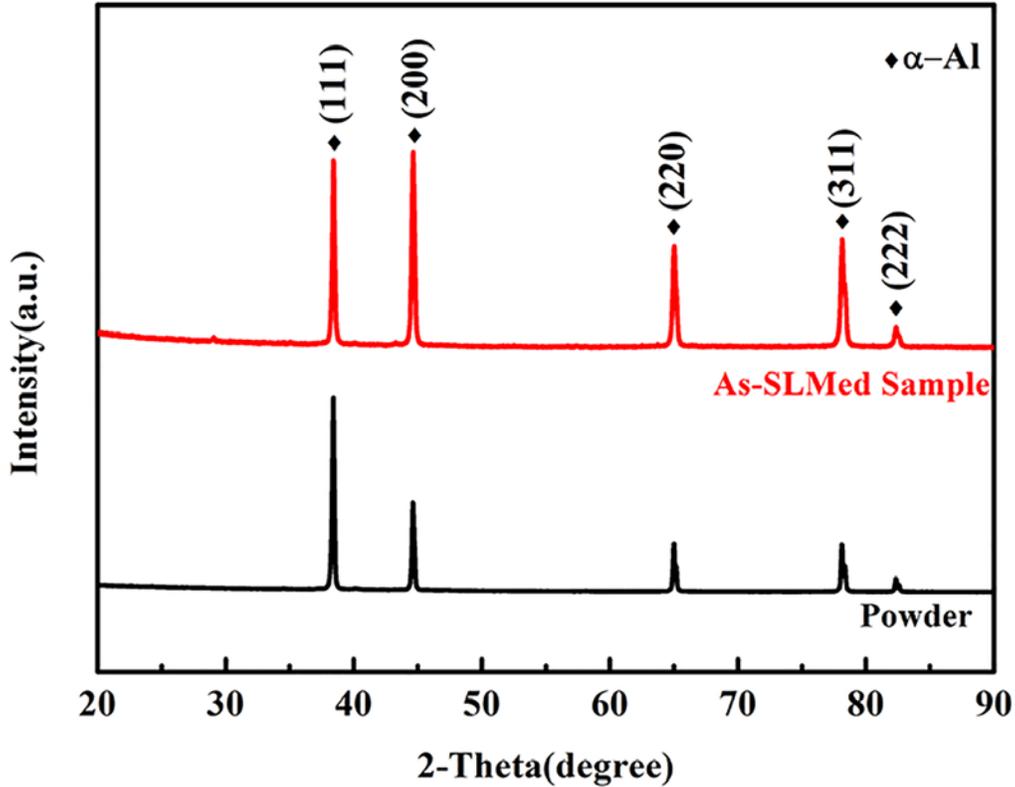
Fig.5. XRD patterns of Al6061 powder and SLM-processed samples.

The SEM micrograph of the 6061 aluminum alloy is shown in Fig. 6. The molten tracks are parallel to each other and overlapped with a clearly visible boundary. Since the laser energy is the Gaussian distribution, the shape of the molten pool is semi-cylindrical and fish scale-like distributed. The width of the molten pool is approximately 180 μm and the depth is about 60 μm. In the SLM process, the temperature at the center line of the molten pool is the highest, and the input heat is dissipated along the vertical direction of the molten tracks, so the grains are epitaxially grown radiated to the boundary of molten pool. Due to the difference in Gaussian heat distribution and solidification mechanism of the laser beam, the microstructure exhibits different characteristics. The high melt temperature and cooling rate inside the molten pool cause the fine and uniform grains, which is called fine grain zone (FGZ). At the boundary of the melt, the laser tracks overlap each other and the grains at the boundary are remelted and resolidified, thus a coarse grain region (CGZ) is formed. Grains outside the boundary of the melt do not undergo remelting during the laser processing but a continuous action of the high temperature with relative low cooling rate for a long time, forming a heat affected zone (HAZ) with coarser grains. There is no obvious precipitation phase in the alloy structure. Non-equilibrium solidification during SLM process enlarges the solid solution limit of the alloy, Mg, Si and other elements are all dissolved in the α-Al matrix. This result is consistent with the XRD phase analysis results. EDS analysis results are shown in the figure.
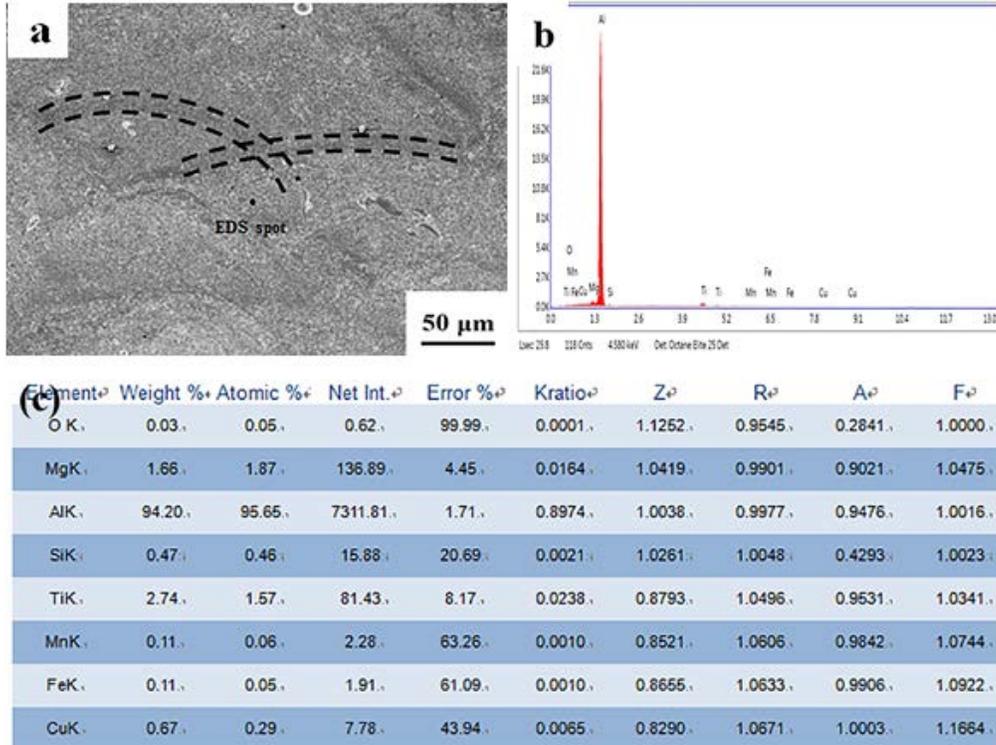
Fig.6. Microstructure and EDS results of SLM 6061 aluminum alloy

The table content from Fig.6(c):

Element	Weight %	Atomic %	Net Int.	Error %	Kratio	Z	R	A	F
O K	0.03	0.05	0.62	99.99	0.0001	1.1252	0.9545	0.2841	1.0000
MgK	1.66	1.87	136.89	4.45	0.0164	1.0419	0.9901	0.9021	1.0475
AlK	94.20	95.65	7311.81	1.71	0.8974	1.0038	0.9977	0.9476	1.0016
SiK	0.47	0.46	15.88	20.69	0.0021	1.0261	1.0048	0.4293	1.0023
TiK	2.74	1.57	81.43	8.17	0.0238	0.8793	1.0496	0.9531	1.0341
MnK	0.11	0.06	2.28	63.26	0.0010	0.8521	1.0606	0.9842	1.0744
FeK	0.11	0.05	1.91	61.09	0.0010	0.8655	1.0633	0.9906	1.0922
CuK	0.67	0.29	7.78	43.94	0.0065	0.8290	1.0671	1.0003	1.1664

Nanohardness

The results of the nanohardness test of SLM-processing Al6061 alloy specimens are shown in Fig. 7. It can be seen that as the laser power increases, the elastic modulus and nanohardness of SLM aluminum alloys increased first and then decreased. From the Fig.7(b), the nanohardness of SLM aluminum alloy parts gradually decreases as the scanning speed increases. In summary, the hardness of SLM aluminum alloy is closely related to the laser energy density.
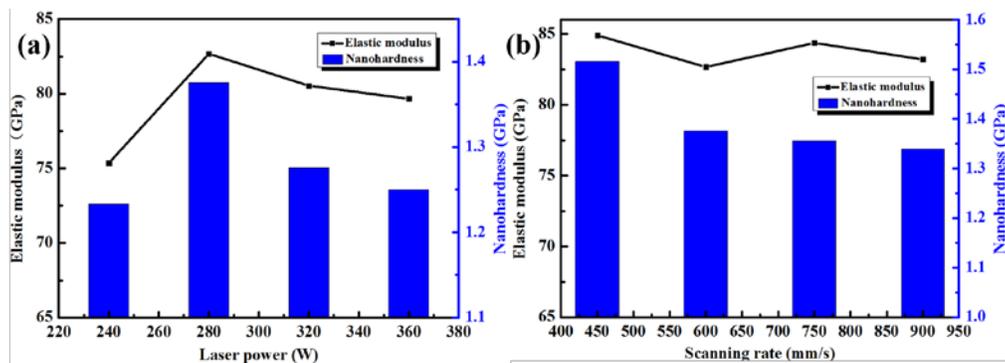
Fig.7. Nanohardness for nano-indentation of samples at different

(b) laser power and (c) scanning rate.

Conclusions

Al6061 alloy has been produced by SLM with different laser power and scanning rate. The main conclusions of the present study, which might be helpful for other laser-powder-based AM technologies and for hard-forming aluminum alloys, are as follows:

1. The increased laser energy density leads to a higher densification level of the SLM processed Al6061 samples. Specimen fabricated with 85 J/mm line energy density has a lowest porosity of 2%.
2. α-Al is the only phase in the raw powder and SLM-processed samples. The relative intensity of α-Al (200) Braggs peak of SLM sample is much stronger than the original powder while the α-Al (111) Braggs peak of SLM sample is weaker than the original powder, which is indicative of the preferable orientation of lattice plane (200) during solidification of α-Al, due to the preferential solidification in the ⟨100⟩ direction.
3. The nanohardness and elastic modulus of SLM-processing Al6061 alloy is closely related to the laser energy density.

Acknowledgements

References

[1] Williams J. C., Jr E. A. S. Progress in structural materials for aerospace systems 1. Acta Mater., 2003, 51: 5775-5799.

[2] A. Heinz, A. Haszler, C. Keidel, et al. Recent development in aluminum alloys for aerospace applications. Mater. Sci. Eng. A, 2000, 280: 102-107.

[3] Tolga Dursun, Costas Soutis. Recent developments in advanced aircraft aluminum alloys. Mater. Design, 2014, 56: 862-871.

[4] E. A. Starke, Jr, J. T. Staley. Application of modern aluminum alloys to aircraft. Progress in Aerospace Sciences, 1996, 32: 131-172.

[5] Steen WM. Laser materials processing. London: Springer, 2003.

[6] Noriko Read, Wei Wang, Khamis Essa, Moataz M. Attallah. Selective laser melting of AlSi10Mg alloy: Process optimisation and mechanical properties development. Mater. Design, 2015, 65: 417–424.

[7] K.G. Prashanth, S. Scudino, H. J. Klauss, K. B. Surreddi, L. Löber, Z. Wang. Microstructure and mechanical properties of Al–12Si produced by selective laser melting: Effect of heat treatment. Mater. Sci. Eng. A, 2014, 590: 153–160.

[8] Wei Li, Shuai Li, Jie Liu. Effect of heat treatment on AlSi10Mg alloy fabricated by selective laser melting: Microstructure evolution, mechanical properties and fracture mechanism. Mater. Sci. Eng. A, 2016, 663: 116–125.

[9] Shafaqat Siddique, Muhammad Imran, Frank Walther. Very high cycle fatigue and fatigue crack propagation behavior of selective laser melted AlSi12 alloy. Inter. J. of Fat., 2017, 94: 246–254.

[10] A. B. Spierings, K. Dawson, T. Heeling, P. J. Uggowitzer, R. Schäublind, F. Palme, K. Wegener. Microstructural features of Sc- and Zr-modified Al-Mg alloys processed by selective laser melting. Mater. Design, 2017, 115: 52–63

[11] Zhang H., Zhu H., Qi T., et al. Selective laser melting of high strength Al–Cu–Mg alloys: Processing, microstructure and mechanical properties. Mater. Sci. Eng. A, 2016, 656: 47-54.

[12] Simchi A, Pohl H. Effect of laser sintering processing parameters on the microstructure and densification of iron powder. Mater. Process Eng., 2003, A359 (1–2): 119–28.

[13] Sanz-Guerrero J, Ramos-Grez J. Effect of total applied energy density on the densification of copper–titanium slabs produced by a DMLF processs. Mater. Process Technol., 2008, 202(1–3): 339–46.